CHAPTER 1

DISSERTATION INTRODUCTION

Introduction

Motivation

Since 1903, the Cu_2MnAl discovered by Fritz Heusler, and it shows ferromagnetic behavior although these constituent elements are non–ferromagnetic thus called "Heusler alloys" (Heusler, Starck & Haupt, 1903, pp.220–223; 1903, pp.219–223). Nowadays, the Heusler alloys composed four families and more than 1000 members, such as half–Heusler (hH, XYZ), full–Heusler (fH, X_2YZ), inverse–Heusler (iH, YX_2Z), and quaternary–Heusler (qH, $XX'YZ$). Where, X, X', and Y are a transition metal and the rare earth element, Z is elements from group 3A–5A, and $X' \neq X$ (Graf, Felser & Parkin, 2011, pp.1–50). The magnetic property of Heusler alloys can be predicted by counting the number of valence electrons (N_{VE}) (Felser, Fecher & Balke, 2007, pp.668–699). For hH alloys, the semiconductor, paramagnetic, and ferromagnetic predicted using the N_{VE} equal to eight or eighteen, seventeen, and nineteen, respectively. The semiconductor, ferromagnetic, and superconductor required the N_{VE} equal to twenty–four, less than twenty–four, and twenty–seven, respectively, for fH, iH, and qH alloys (Graf et al., 2011, pp.1–50). Besides, Buschow and Engen (1981, pp.90–96) reported the fH used entirely in the magneto–optic materials. In addition, Heusler alloys widely applied in spintronic device (Nikolaev et al., 2009, p.222501), spin torque device (Wu et al., 2009, p.122503), superconductors (Wernick et al., 1983, pp.90–92), topological insulators (Graf et al., 2011, pp.1–50), and

thermoelectric materials (Asahi, Morikawa, Hazama & Matsubara, 2008, p.064227). The thermoelectric (TE) is alternative energy and more important in recent years. TE materials can convert a temperature from waste heat into electricity. The performance of TE materials can be considered using the dimensionless figure of merit; $ZT = S^2\sigma T/\kappa$, where S is the Seebeck coefficient, σ is electrical conductivity, κ is thermal conductivity, and T is absolute temperature (Aswal, Basu & Singh, 2016 pp. 50–67). The high ZT of Heusler compounds mostly found in hH with N_{VE} = 18. Aswal et al. (2016, pp. 50–67) proposed the high ZT of TiNiSn–based hH at intermedium–temperature range. The TiNiSn is an *n*–type TE material with high ZT value of ~0.3 – 0.4 at 600 – 800 K (Cook & Harringa, 1999, pp. 323–327; Kim, Kimura & Mishima, 2007, pp. 349–356; Muta, Kanemitsu, Kurosaki & Yamanaka, 2009, pp. 50–55). The TiNiSn advantage is low cost, earth–abundant materials, high melting point (1970 K), and high thermal stability (Berry et al., 2017, pp. 1543–1550; Bankina, Fedorova & Leytus, 1993; Muta et al., 2009, pp. 50–55). In TE property, TiNiSn shows narrow band gap value of ~0.1 – 0.6 eV, large S about –350 μV K^{-1}, low electrical resistivity ($\rho = 1/\sigma$) ~0.1 – 8 mΩ cm (Bhattacharya et al., 1999, pp. 336–339; Kim et al., 2007, pp. 349–356; Bhattacharya et al., 2008, p. 184203; Berry et al., 2017, pp. 1543–1550) at room temperature. However, the TiNiSn disadvantage is high κ. Therefore, the ZT of TiNiSn less than the conventional TE materials (Bhattacharya et al., 1999, pp. 336–339; Kim et al., 2007, pp. 349–356). From the ZT equation, high ZT required a high power factor ($S^2\sigma$) and a low κ. Several research works used the alloy scattering, defect phonon scattering and nanostructure method to reduce the κ (Bhattacharya et al., 1999, pp. 336–339; Gürth et al., 2016, pp. 210–222; Katayama, Kim, Kimura & Mishima, 2003, pp.1160–1165. In electrical part, it can be improved the power factor by tuning the carrier concentration, such as band structure engineering, tuning a carrier concentration, and increasing crystal complexity

(Katayama et al., 2003, pp.1160–1165; Kim et al., 2007, pp. 349–356; Muta et al., 2009, pp. 50–55; Berry et al., 2017, pp. 1543–1550; Yang, Chen, Meisner & Uher, 2002; Douglas et al., 2014, pp. 043720). From above mentioned, the theoretical thermoelectric property of TiNiSn still lacks in detail.

This dissertation presented the theoretical investigation of the thermoelectric property of TiNiSn–based hH alloys. The density functional theory–based with the Boltzmann transport equation (BTE) and quasi–harmonic Debye model performed to calculate the electronic structure, thermal property, and TE property. Chapter 1 is an introduction, the literature review, and related theory. Chapter 2 presents a topic "enhancing the thermoelectric performance of self–defect TiNiSn: a first–principles calculation". Chapter 3 presents a topic "reduced lattice thermal conductivity of Ti–site substituted transition metals $Ti_{1-X}TM_XNiSn$ a quasi–harmonic Debye model study". Chapter 4 presents a topic "enhancing the thermoelectric properties of TiNiSn by transition metals co–doped on the Ti–site of $Ti_{0.5}TMI_{0.25}TMII_{0.25}NiSn$: A first–principles study". Chapter 5 presents a topic "First–principles investigation on thermoelectric properties of $TiNiSn_{1-x}A_x$ (A = As, Sb, Bi; x = 0 – 0.125) half–Heusler alloys". The structure of chapters 2 – 5 composed introduction, computational details, results and discussion, and summary. The conclusion illustrated in Chapter 6. Chapters 2 – 4 carried out at the Simulation Research Laboratory (SRL), Center of Excellence on Alternative Energy (CEAE), Sakon Nakhon Rajabhat University, Sakon Nakhon, Thailand. Chapter 5 carried out at Diño Research Group, Department of Applied Physics, Graduate School of Engineering, Osaka University, Osaka, Japan.

Objectives

1. To investigate the electronic structure of Sc, Zr, Hf, Nb, V, Mn, As, Sb, and Bi dope TiNiSn by using the density functional theory–based.

2. To investigate the thermoelectric properties of Sc, Zr, Hf, Nb, V, Mn, As, Sb, and Bi dope TiNiSn by using the density functional theory–based.

Anticipated outcomes of the dissertation

1. Obtained the electronic and thermoelectric property of Sc, Zr, Hf, Nb, V, Mn, As, Sb, and Bi dope TiNiSn half Heusler alloys.

2. Obtained the optimal candidate for enhancing the thermoelectric properties of Ti–Ni–Sn half Heusler alloys.

Theoretical Background

Heusler alloys

Heusler alloys are a large group which more than 1000 members and its wide range of material property. The element predict table for Heusler alloys illustrated in Figure 1 (Graf et al., 2011, pp.1–50). Heusler alloys have a face–centered cubic (FCC) crystal structure with two different compositions. One is a ternary composition, 1:1:1 for hH. Two is a quaternary composition, such as 2:1:1 for fH, 1:2:1 for iH, and 1:1:1:1 for qH, respectively. The Heusler alloys crystal structure data illustrated in Figure 2 and Table 1.

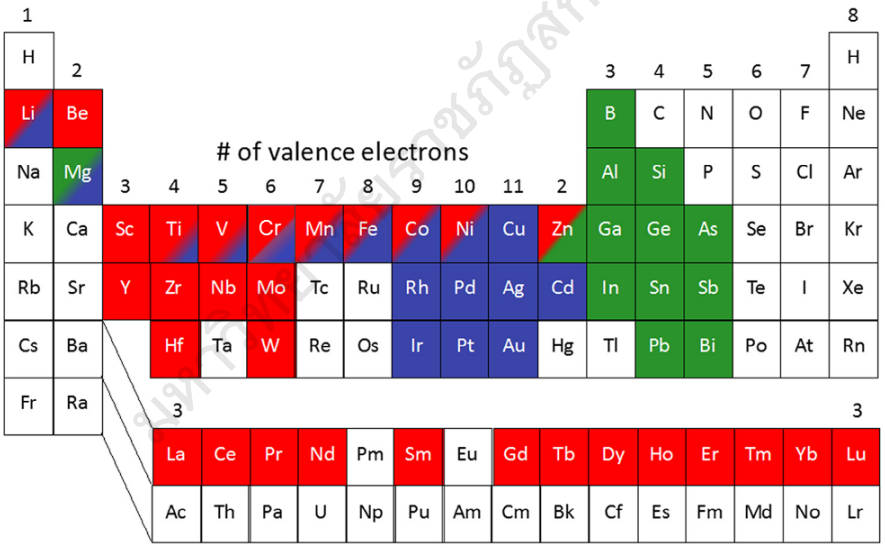

Figure 1 Periodic table for Heusler compounds. Blue, red, and green color are representing an element for *X*, *Y*, and *Z*, respectively.

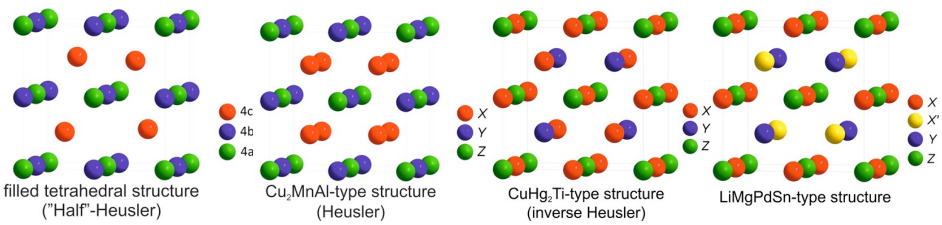

Figure 2 The family of Heusler structure composed hH, fH, iH, and qH.

Table 1 The Heusler alloys crystal structure data.

	Space group number	4a (0,0,0)	4b (1/2, 1/2, 1/2)	4c (1/4, 1/4, 1/4)	4d (3/4, 3/4, 3/4)
half Heusler[1]	216	*X*	*Z*	*Y*	
full Heusler[1]	225	*Y*	*Z*	*X*	*X*
inverse Heusler[1]	216				
type I		*X*	*Y*	*Z*	
type II		*Z*	*X*	*Y*	
type III		*Y*	*Z*	*X*	
quaternary Heusler[2]	216				
type I		*X*	*Y*	*X'*	*Z*
type II		*X*	*X'*	*Y*	*Z*
type III		*X*	*Z*	*X'*	*Y*

(1) Graf et al., 2011, pp.1–50

(2) Yan et al., 2016, pp.64–67

Slater and Pauling (Slater, 1936, p.537; Pauling, 1938, p.899) estimated the magnetic moment (m) from the average N_{VE} per atoms. The magnetic moment in multiples of Bohr magnetrons μ_{B}) is given by an equation;

$$m = N_{\mathrm{VE}} - 2n_{\downarrow}, \tag{1}$$

where $2n_{\downarrow}$ is the number of electrons in the minority states. In the case of hH alloys, the Slater–Pauling rule is given by an equation;

$$m_{XYZ} = N_{\mathrm{VE}} - 18. \tag{2}$$

For fH, iH, and qH alloys, the Slater–Pauling rule is given by an equation;

$$m_{X_2YZ} = m_{YX_2Z} = m_{XX'YZ} = N_{\mathrm{VE}} - 24. \tag{3}$$

The m per formula unit as a function of the N_{VE} presents in Figure 3.

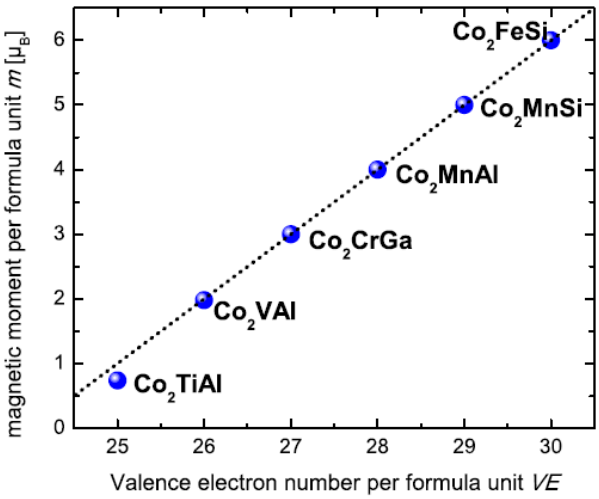

Figure 3 The magnetic moment per formula unit of Co_2–based fH alloys agree with the Slater–Pauling rule.

Theorem of thermoelectricity

The TE phenomena with an energy conversion from heat to electricity can be conveniently discussed regarding the schematic of a thermocouple, as shown in Figure 4. It can be considered as a circuit formed from two dissimilar conductors. From Figure 4, a and b are connected electrically in series but thermally in parallel. If the junctions A and B are maintained at different temperatures T_1 and T_2, $T_1 > T_2$ is an open circuit electromotive force (emf). V is developed between C and D gave by $V = S(T_1 - T_2)$ or $S = V/\Delta T$. Therefore, the differential Seebeck coefficient S_{ab} defines between the elements a and b. The relationship is linear for small temperature differences. The sign of a is positive if the emf causes the current to flow in a clockwise direction around the circuit and is measured in V K^{-1}.

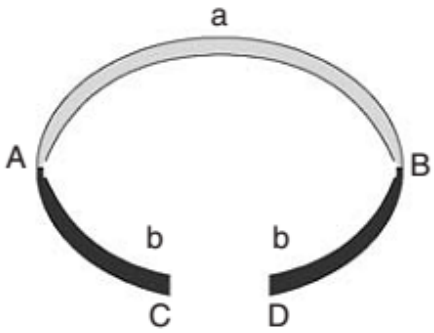

Figure 4 Schematic primary thermocouple (Rowe, 2006, p. 1–1).

For Peltier effect, in Figure 4, the reverse situation is considered with an external emf source applied across C and D. A current I flows in a clockwise sense around the circuit. A rate of heating q occurs at one junction between a and b. A rate of cooling $-q$ occurs at the other. The ratio of I to q defines the Peltier coefficient (Π) given by $\Pi = I/q$, and this is positive if A is heated, B is cooled, and is measured in watts per ampere or volts.

The Thomson effect relates to the rate of generation of reversible heat q, which results from the passage of current along a portion of a single conductor, along which there is a temperature difference ΔT. Providing the temperature difference is small, $q = \beta I \Delta T$, where β is the Thomson coefficient. The units of β are the same as those of the Seebeck coefficient V K^{-1}. Although the Thomson effect is not of primary importance in thermoelectric devices, it should not be neglected in detailed calculations.

The efficiency of the TE material included of the TE generator (η) and TE cooler efficiency (COP) with:

$$\eta = \frac{T_\mathrm{H} - T_\mathrm{C}}{T_\mathrm{H}} \left(\frac{\sqrt{1+Z\bar{T}}-1}{\sqrt{1+Z\bar{T}}+T_\mathrm{C}/T_\mathrm{H}} \right), \tag{4}$$

$$\mathrm{COP} = \frac{(ZT_\mathrm{H}^2/2)-\Delta T}{ZT_\mathrm{H}T_\mathrm{C}}, \tag{5}$$

where, the subscript H and C are hot and cold temperature, and ΔT is difference temperature. $\bar{T}$ is average temperature. The relation between ZT and efficiency, for example, ZT and η presented in Figure 5.

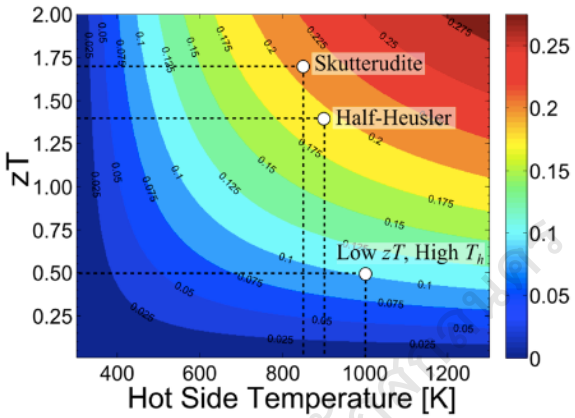

Figure 5 The relation of ZT and η versus hot side temperature for skutterudite, hH, and low ZT material (Snyder & Toberer, 2008, pp. 105–114).

From above mentioned in a motivation section, the equation $ZT = S^2\sigma T/\kappa$ means TE property depended on temperature. Besides, TE property also depended on the electronic structure like carrier concentration with:

$$S = \frac{8\pi^2 k_B^2}{3e\mathrm{h}^2} m^* T \left(\frac{\pi}{3n}\right)^{2/3}, \tag{6}$$

$$\sigma = ne\mu, \tag{7}$$

where, n is a carrier concentration, m^* is an effective mass, h is the Plank's constant, e is an electron charge, k_B is the Boltzmann's constant, and μ is carrier mobility. The κ includes the electron part and lattice or phonon part given by:

$$\kappa = \kappa_e + \kappa_l = ne\mu LT + \frac{1}{3} C_V v_T l, \tag{8}$$

where κ_e is electron thermal conductivity, κ_l is a lattice thermal conductivity, C_V is heat capacity at constant volume, v_T is a sound velocity depend on

temperature, L is the Lorenz number, and l is a phonon mean free path. The optimal TE property can be improved by tuning carrier concentration as shown in Figure 6. Figure 7 shows the ZT versus temperature for n–type and p–type TE materials. So, the TE materials can be applied in low–, intermedium–, and high–temperature range depend on the specific materials.

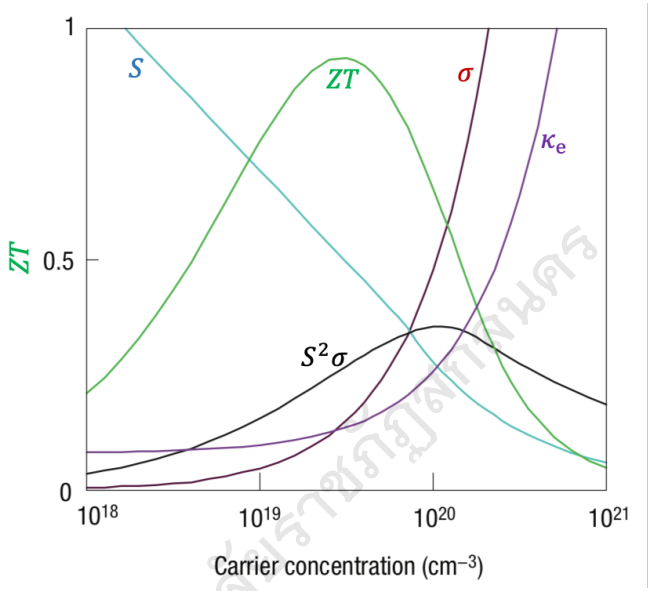

Figure 6 Thermoelectric properties versus carrier concentration.

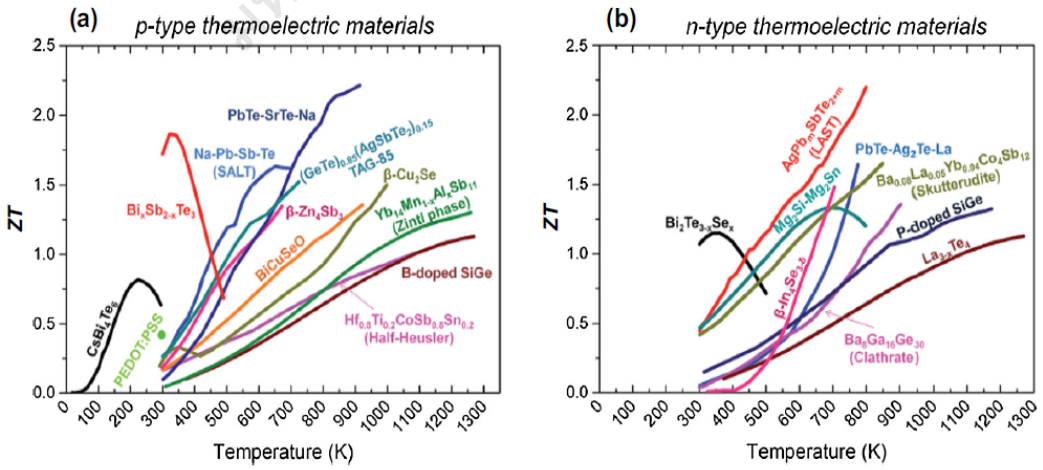

Figure 7 The ZT versus temperature for (a) p–type and (b) n–type thermoelectric materials.

Density functional theory

Modern computational modeling of materials from first-principles trusted on a theoretical and computational technique. These techniques based on the density functional theory (DFT). DFT is a method for examining molecules, nanostructures, solids, surfaces, and interfaces through the directly unraveling approximate of the Schrödinger equation. Figure 8 shows the records to Hohenberg and Kohn's article (Hohenberg & Kohn, 1964, pp. 864–867; p. B864). These records have been increasing steadily at a rapid step since the 1960s.

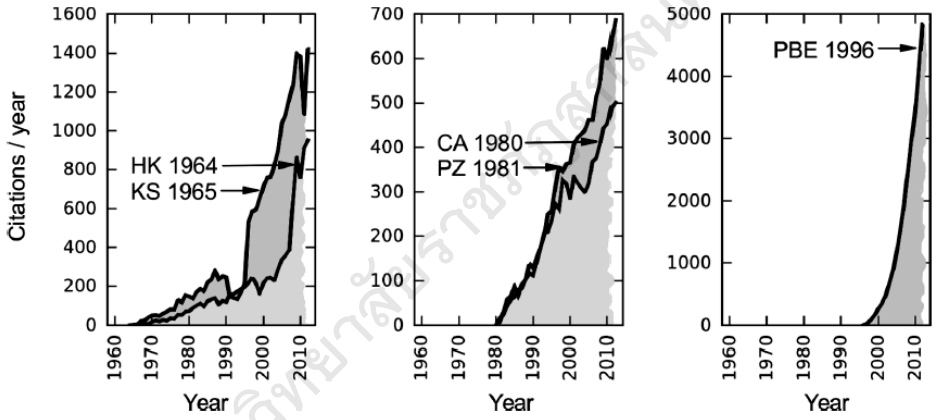

Figure 8 A statistic of citation per year to the DFT works (Giustino, 2014).

The DFT starts from the many-body Schrödinger equation to Hartree-Fock equation (Fock, 1930, pp. 126–148; Hartree, 1928, pp. 89–110), Kohn-Sham equation (Khon & Sham, 1965, p. A1133) as well as self-consistent calculation (Hohenberg & Kohn, 1964, pp. 864–867; p. B864). The time-independent Schrödinger equation yields the following symbolic form:

$$(\text{kinetic energy} + \text{potential energy})\psi = E_{\text{tot}}\psi, \qquad (9)$$

where E_{tot} is the total energy for the wavefunction ψ . The probability of finding the particle at the point $\mathbf{r}$ is $|\psi(\mathbf{r})|^2$. For one electron, the potential energy $V(\mathbf{r})$, equation (9) can be written as:

$$\left(\frac{\mathbf{p}^2}{2m_e} + V(\mathbf{r})\right)\psi(\mathbf{r}) = E_{\mathrm{tot}}\psi(\mathbf{r}), \tag{10}$$

where m_e is an electron mass, and $V(\mathbf{r})$ is a potential energy function. The quantum–mechanical momentum operator is given by:

$$\mathbf{p} = -i\hbar\nabla, \nabla = \mathbf{u}_x\frac{\partial}{\partial x} + \mathbf{u}_y\frac{\partial}{\partial y} + \mathbf{u}_z\frac{\partial}{\partial z}, \tag{11}$$

where $\hbar$ is the Dirac constant. The ψ_0 is the lowest–energy solution of an equation (10). At equilibrium the system in lowest–energy configuration, for example the electron occupies the state ψ_0 accurately. The electron charge distribution at equilibrium is therefore given by $|\psi_0(\mathbf{r})|^2$. The integral of the electronic charge density during the material yields the number of electrons, N:

$$N = \int \rho(\mathbf{r})d\mathbf{r}, \tag{12}$$

where $\rho(\mathbf{r})$ is the electron density which simple evaluate by $n(\mathbf{r}) = \sum\int|\psi(\mathbf{r})|^2 d\mathbf{r}$.

The E_{tot} of the system in the quantum state was specified by the many–body wavefunction Ψ, where $\Psi = \Psi(\mathbf{r}_i, \mathbf{R}_i)$ and $i = 1, 2, \ldots, N$. The kinetic and potential energy for N electrons and M nuclei can be written as:

$$\text{kinetic energy} = -\sum_{i=1}^{N}\frac{\hbar^2}{2m_e}\nabla_i^2 - \sum_{I=1}^{M}\frac{\hbar^2}{2M_I}\nabla_I^2 , \tag{13}$$

where $M_I = M_1, M_2, \ldots$ is a mass of nuclei, and ∇^2 is the Laplace operator. The potential term can be express as:

$$(\text{potential energy})_{\mathrm{ee}} = \frac{1}{2}\sum_{i\neq j}^{N}\frac{e^2}{4\pi\epsilon_0}\frac{1}{|\mathbf{r}_i - \mathbf{r}_j|} , \tag{14}$$

$$(\text{potential energy})_{\mathrm{nn}} = \frac{1}{2}\sum_{I\neq J}^{N}\frac{e^2}{4\pi\epsilon_0}\frac{Z_I Z_J}{|\mathbf{R}_I - \mathbf{R}_J|} , \tag{15}$$

$$(\text{potential energy})_{\mathrm{en}} = \sum_{i,I}^{N}\frac{e^2}{4\pi\epsilon_0}\frac{Z_I}{|\mathbf{r}_i - \mathbf{R}_I|} . \tag{16}$$

The many–body Schrödinger equation is written as:

$$\left[-\sum_{i=1}^{N}\frac{\hbar^2}{2m_e}\nabla_i^2 \;-\sum_{I=1}^{M}\frac{\hbar^2}{2M_I}\nabla_I^2 \;+\frac{1}{2}\sum_{i\neq j}^{N}\frac{e^2}{4\pi\epsilon_0}\frac{1}{|\mathbf{r}_i-\mathbf{r}_j|} + \frac{1}{2}\sum_{I\neq J}^{N}\frac{e^2}{4\pi\epsilon_0}\frac{Z_I Z_J}{|\mathbf{R}_I-\mathbf{R}_J|} + \frac{1}{2}\sum_{i,I}^{N}\frac{e^2}{4\pi\epsilon_0}\frac{Z_I}{|\mathbf{r}_i-\mathbf{R}_I|}\right]\Psi(\mathbf{r}) = E_{\text{tot}}\Psi(\mathbf{r}). \tag{17}$$

In Hartree atomic units, the many–body Schrödinger equation obtained from:

$$\left[-\sum_i\frac{\nabla_i^2}{2}-\sum_I\frac{\nabla_I^2}{2M_I}+\sum_{i,I}\frac{Z_I}{|\mathbf{r}_i-\mathbf{R}_I|}+\frac{1}{2}\sum_{i\neq j}\frac{1}{|\mathbf{r}_i-\mathbf{r}_j|} + \frac{1}{2}\sum_{I\neq J}\frac{Z_I Z_J}{|\mathbf{R}_I-\mathbf{R}_J|}\right]\Psi(\mathbf{r}) = E_{\text{tot}}\Psi(\mathbf{r}). \tag{18}$$

The nuclear coordinates disappear completely as:

$$\left[-\sum_i\frac{\nabla_i^2}{2}+\sum_i V_{\text{n}}(\mathbf{r})+\frac{1}{2}\sum_{i\neq j}\frac{1}{|\mathbf{r}_i-\mathbf{r}_j|}\right]\Psi = E\Psi. \tag{19}$$

The simple Kohn–Sham equation for single particle can be written as:

$$\left[-\frac{\nabla^2}{2}+V_{\text{n}}(\mathbf{r})+V_{\text{H}}(\mathbf{r})+V_x(\mathbf{r})+V_c(\mathbf{r})\right]\phi_i(\mathbf{r}) = \varepsilon_i\phi_i(\mathbf{r}), \tag{20}$$

where V_{H} is Hartree–Fock potential, V_x is exchange–potential, and V_c is correlation potential. The many–electron Hamiltonian can be written as:

$$\mathbf{H}(\mathbf{r}_1,\mathbf{r}_2,\dots,\mathbf{r}_N) = -\sum_i\frac{\nabla_i^2}{2}+\sum_i V_{\text{n}}(\mathbf{r})+\frac{1}{2}\sum_{i\neq j}\frac{1}{|\mathbf{r}_i-\mathbf{r}_j|}. \tag{21}$$

The energy, E, of this state is obtain by:

$$E = \langle\Psi^*|\mathbf{H}|\Psi\rangle = \int \mathrm{d}\mathbf{r}_1,\mathrm{d}\mathbf{r}_2,\dots,\mathrm{d}\mathbf{r}_N\,\Psi^*(\mathbf{r}_1,\mathbf{r}_2,\dots,\mathbf{r}_N)\mathbf{H}\Psi(\mathbf{r}_1,\mathbf{r}_2,\dots,\mathbf{r}_N). \tag{22}$$

The DFT concept is an observation that if E is the lowest possible energy of the system. For example, the energy of the ground state, then E is a functional of the electron density, $F[\rho]$:

$$E = F[\rho]. \tag{23}$$

The total energy of a many–electron system is a functional of the $n(\mathbf{r})$ drives under the Hoenberg–Kohn theorem (Hohenberg & Kohn, 1964, pp. 864–867; p. B864). The proof is based on the following three premises:

i) In the ground state, the $n(\mathbf{r})$ determines the external potential of the nuclei, V_n, in equation (21): $\rho \rightarrow V_n$.

ii) In any quantum state, the V_n, determines the many–electron wavefunction: $V_n \rightarrow \Psi$.

iii) In any quantum state, E is a functional of the many–body wavefunction through equation (1.22): $\Psi \rightarrow E$.

It indicates that the E must be a functional of the density: $E = F[\rho]$. However, the exact form of this functional is still unknown. Since the original work by Hohenberg and Kohn, a number of very useful approximations have been developed. Equation (24) can certainly rewrite this functional as follows:

$$F[\rho] = \int \mathrm{d}\mathbf{r}\rho(\mathbf{r})V_n(\mathbf{r}) + \langle\Psi[\rho]|\mathbf{T} + \mathbf{W}|\Psi[\rho]\rangle. \tag{24}$$

$$F[\rho] = \int \mathrm{d}\mathbf{r}\rho(\mathbf{r})V_n(\mathbf{r}) - \sum_i \int d\mathbf{r}\phi_i^*(\mathbf{r})\frac{\nabla^2}{2}\phi_i(\mathbf{r}) + \frac{1}{2}\iint \mathrm{d}\mathbf{r}d\mathbf{r}'\frac{\rho(\mathbf{r})\rho(\mathbf{r}')}{|\mathbf{r}-\mathbf{r}'|} + E_{xc}[\rho] \tag{25}$$

From equation (25), first term is an external potential, second term is a kinetic energy, third term is the Hartree energy, and final term is an exchange–correlation energy. It turns out that the ground–state density, n_0, is precisely the function that minimizes $E = F[\rho]$. This property is called the "Hohenberg–Kohn variational principle" and can be expressed as follows (Hohenberg & Kohn, 1964, pp. 864–867; p. B864):

$$\left.\frac{\delta F[\rho]}{\delta n}\right|_{n_0} = 0\,. \tag{26}$$

The exchange and correlation potential as equation (1.21) can be combined and rewritten as $V_{xc}(\mathbf{r})$, and then it is given by;

$$V_{xc}(\mathbf{r}) = \left.\frac{\delta E_{xc}[\rho]}{\delta\rho}\right|_{n(\mathbf{r})}. \tag{27}$$

The $E_{xc}[n]$ is only one approximated parameter in the DFT calculation. The local density approximation (LDA) was formulated by Khon and Sham (Khon & Sham, 1965, p. A1133) which is demonstrated as:

$$E_{xc}^{\mathrm{LDA}}[n] = \iiint \mathrm{d}^3\mathbf{r}\varepsilon_{xc}[\rho]. \tag{28}$$

The $\varepsilon_{xc}[n]$ is exchange–correlation energy per electron based on the assumption that the $E_{xc}^{\mathrm{LDA}}[n]$ is purely local. It can be written into a simple form of the free electron gas model as:

$$\varepsilon_{xc}[\rho] \cong -\frac{3e^2}{2\pi}[3\pi^2\rho(\mathbf{r})]^{1/3}\rho(\mathbf{r}). \tag{29}$$

Nowadays, Chachiyo (2016, p. 021101) have developed the ε_c as equation:

$$\varepsilon_c = a\ln\left(1+\frac{b}{r_s}+\frac{b}{r_s^2}\right). \tag{30}$$

The parameter a and b are not from empirical fitting to the Monte Carlo data, but from the theoretical constant that the functional approaches high–density limit. The Chachiyo's formula is more accurate than the standard VWN fit function (Fitzgerald, 2016, p.20) as shown in Figure 9.

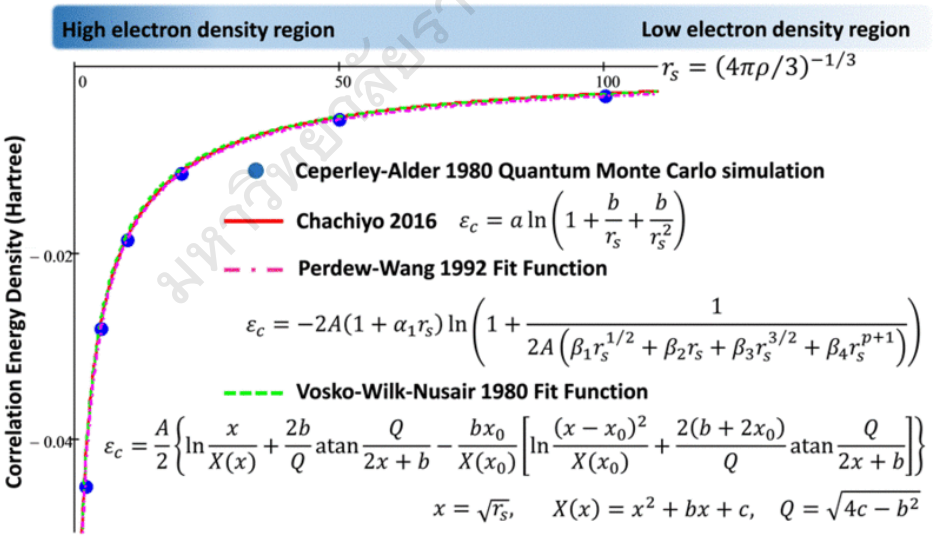

Figure 9 The Chachiyo's formula compared with the Monte Carlo results and VWN functional, and high–density limit Chachiyo (2016, p. 021101).

In addition, the LDA was improved by taken the density gradient, $\nabla\rho(\mathbf{r})$ and called the generalized gradient approximation or GGA. In GGA, the $\varepsilon_{xc}[\rho]$ can be written as:

$$E_{xc}^{\mathrm{GGA}}[\rho] = \iiint \mathrm{d}^3\mathbf{r}\varepsilon_{xc}[\rho]f[\rho(\mathbf{r}), \nabla\rho(\mathbf{r})], \tag{31}$$

where f is function contains an analytic function fitted to particular system.

In order to actually solve the Kohn–Sham equations as well as calculate the total energy, it is convenient to rewrite here the Kohn–Sham equations and each term appearing in them:

$$\left[-\tfrac{1}{2}\nabla^2 + V_{\mathrm{tot}}(\mathbf{r})\right]\phi_i(\mathbf{r}) = \varepsilon_i\phi_i(\mathbf{r}), \tag{32}$$

$$V_{\mathrm{tot}}(\mathbf{r}) = V_{\mathrm{n}}(\mathbf{r}) + V_{\mathrm{H}}(\mathbf{r}) + V_{xc}(\mathbf{r}), \tag{33}$$

$$V_{\mathrm{n}}(\mathbf{r}) = -\sum_I \frac{Z_I}{|\mathbf{r}_i - \mathbf{R}_I|}, \tag{34}$$

$$\nabla^2 V_{\mathrm{H}}(\mathbf{r}) = -4\pi\rho(\mathbf{r}), \tag{35}$$

$$V_{xc}(\mathbf{r}) = \frac{\delta E_{xc}[\rho]}{\delta n}(\mathbf{r}), \tag{36}$$

$$\rho(\mathbf{r}) = \sum_i |\phi_i(\mathbf{r})|^2. \tag{37}$$

The practical procedure for solving the Kohn–Sham equations, it starts by specifying the nuclear coordinates. To solve equation (33) using V_{n} as a first approximation to V_{tot}; however, this is too crude an approximation, and it is more convenient to guess a possible $\rho(\mathbf{r})$, in order to determine a preliminary approximation to the Hartree and exchange and correlation potentials. A simple but very useful approximation is to construct the first guess for the $n(\mathbf{r})$ by adding up the densities corresponding to completely isolated atoms but arranged in the atomic positions corresponding to the material under consideration. Using the density we obtain initial estimates of the $V_{\mathrm{H}} + V_{xc}$, and from there the V_{tot}, needed in equation (33). At this point, it can proceed with the numerical solution of the Kohn–Sham equations. It can be done for example by discretizing the space into a mesh of points

and representing the Laplace operator using finite difference formulas. By solving the Kohn–Sham equations, it can obtain the new ϕ_i, which can be used to construct a better estimate of the ρ and the V_{tot}. This process is then repeated until the new density matches the old density within a desired tolerance, at which point we say that we have achieved self–consistency. The self–consistent procedure illustrated in Figure 10.

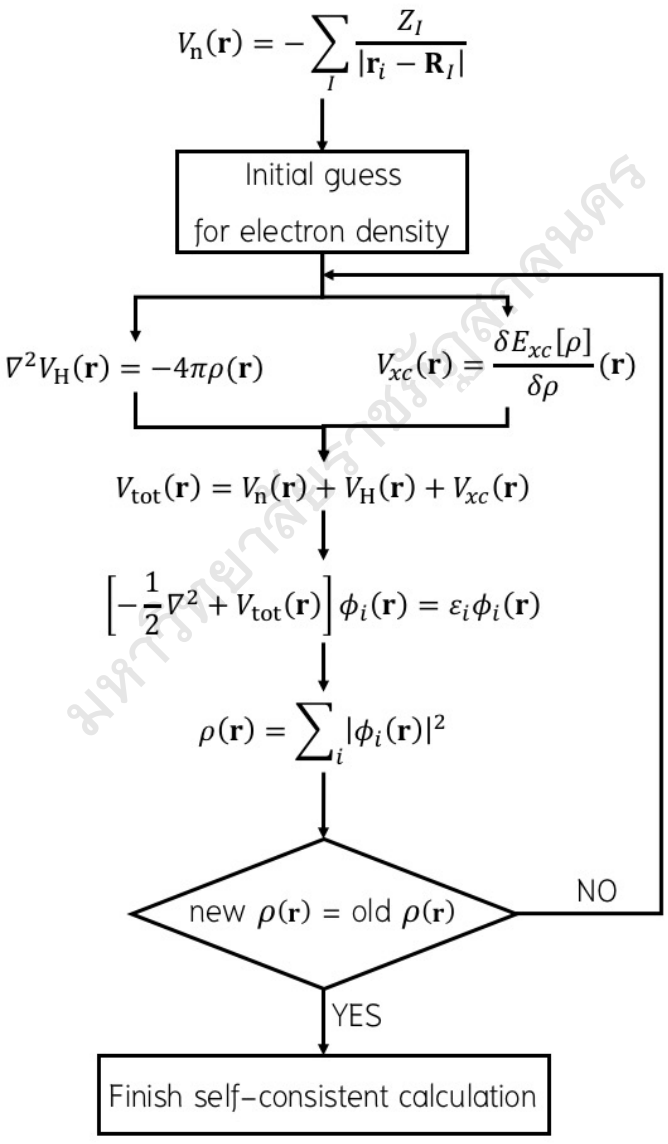

Figure 10 Schematic flow–chart for finding the self–consistent solutions of the Khon–Sham equations.

Boltzmann transport equation

Boltzmann transport theory (Madsen & Singh, 2006, pp.67–71) is a tool for achievement understanding into the transport property of real materials. In the occurrence of an electric– and magnetic–field and a thermal gradient the electric current (J), can be written concerning the conductivity tensors:

$$J_i = \sigma_{ij}E_j + \sigma_{ijk}E_jB_k + v_{ij}\nabla_j T + \cdots \ . \tag{38}$$

In term of the group velocity can be written as:

$$\bar{v}_\alpha(i,\mathbf{k}) = \frac{1}{\hbar}\frac{\partial \varepsilon_{i,\mathbf{k}}}{\partial k_\alpha}, \tag{39}$$

and the inverse mass tensor is

$$M^{-1}_{\beta u}(i,\mathbf{k}) = \frac{1}{\hbar^2}\frac{\partial^2 \varepsilon_{i,\mathbf{k}}}{\partial k_\alpha \partial k_u} \ , \tag{40}$$

the conductivity tensors can be obtained as:

$$\sigma_{\alpha\beta}(i,\mathbf{k}) = e^2\tau_{i,\mathbf{k}}v_\alpha(i,\mathbf{k})v_\beta(i,\mathbf{k}), \tag{41}$$

where $\sigma_{\alpha\beta\gamma}$ is elegantly written using the Levi–Civita symbol, ϵ_{ijk} (Hurd, 2012; Oberkampf, Trucano & Hirsch, 2004, pp. 345–384):

$$\sigma_{\alpha\beta\gamma}(i,\mathbf{k}) = e^3\tau^2_{i,\mathbf{k}}\epsilon_{\gamma uv}v_\alpha(i,\mathbf{k})v_v(i,\mathbf{k})M^{-1}_{\beta u}. \tag{42}$$

The notation used in equations (42) – (43) the symmetry of the conductivity tensors directly. In an orthorhombic symmetry, $\sigma_{\alpha\beta}$ is diagonal with all three components independent, and $\sigma_{\alpha\beta\gamma}$ has three independent components and vanishes unless α, β, and γ are all different. The relaxation time, τ, in principle is dependent on both the band index and the $\mathbf{k}$ vector direction. However detailed studies of the direction dependence of τ have shown that, to a good approximation, τ is direction independent (Schulz Allen & Trivedi, 1992) and that even in the superconducting cuprates, that have substantially anisotropic conduction and cell–axes, the τ is almost isotropic (Allen, Pickett & Krakauer, 1988, p. 7482). In the present we will use the simplest approximation for the relaxation time, namely to keep it constant,

which is the most often used in praxis. Similar to the density of states energy projected conductivity tensors can be defined using the conductivity tensors, equations. (41) – (42)

$$\sigma_{\alpha\beta}(\varepsilon) = \frac{1}{N_k}\sum_{i,\mathbf{k}} \sigma_{\alpha\beta}(i,\mathbf{k})\,\frac{\delta(\varepsilon-\varepsilon_{i,\mathbf{k}})}{\mathrm{d}\varepsilon}, \tag{43}$$

where N_k is the number of $\mathbf{k}$–points sampled. Similarly, $\sigma_{\alpha\beta\gamma}(\varepsilon)$ can be defined. The transport tensors, equation (38), can then be calculated from the conductivity distributions

$$\sigma_{\alpha\beta}(T;\mu_{\text{chem.}}) = \frac{1}{\Omega}\int \sigma_{\alpha\beta}(\varepsilon)\left[-\frac{\partial f_{\mu_{\text{chem.}}(T;\varepsilon)}}{\partial\varepsilon}\right]\mathrm{d}\varepsilon, \tag{44}$$

$$v_{\alpha\beta}(T;\mu_{\text{chem.}}) = \frac{1}{eT\Omega}\int \sigma_{\alpha\beta}(\varepsilon)(\varepsilon-\mu_{\text{chem.}})\left[-\frac{\partial f_{\mu_{\text{chem.}}(T;\varepsilon)}}{\partial\varepsilon}\right]\mathrm{d}\varepsilon, \tag{45}$$

$$\kappa^0_{\alpha\beta}(T;\mu_{\text{chem.}}) = \frac{1}{e^2T\Omega}\int \sigma_{\alpha\beta}(\varepsilon)(\varepsilon-\mu_{\text{chem.}})^2\left[-\frac{\partial f_{\mu_{\text{chem.}}(T;\varepsilon)}}{\partial\varepsilon}\right]\mathrm{d}\varepsilon, \tag{46}$$

$$\sigma_{\alpha\beta\gamma}(T;\mu_{\text{chem.}}) = \frac{1}{\Omega}\int \sigma_{\alpha\beta\gamma}(\varepsilon)\left[-\frac{\partial f_{\mu_{\text{chem.}}(T;\varepsilon)}}{\partial\varepsilon}\right]\mathrm{d}\varepsilon, \tag{47}$$

where $\boldsymbol{\kappa^0}$ is the electronic part of the thermal conductivity. The Seebeck and Hall coefficients can then easily be calculated

$$S_{ij} = E_i\left(\nabla_j T\right)^{-1} = (\sigma^{-1})_{\alpha i} v_{\alpha j}, \tag{48}$$

$$R_{ijk} = \frac{E_j^{\text{ind}}}{J_i^{\text{appl}} B_k^{\text{appl}}} = (\sigma^{-1})_{\alpha j}\sigma_{\alpha\beta k}(\sigma^{-1})_{i\beta}. \tag{49}$$

Under the assumption that the relaxation time τ is direction independent, both the Seebeck and the Hall coefficients are independent of τ.